

Fig. 3

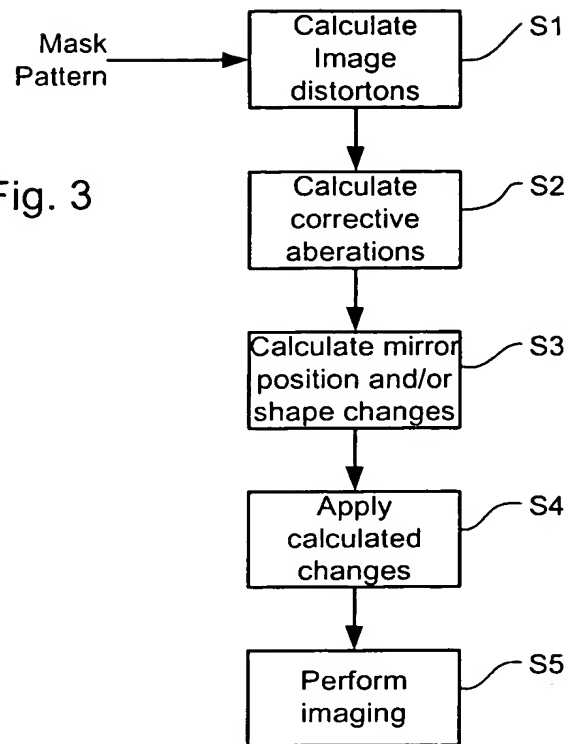


Fig. 4

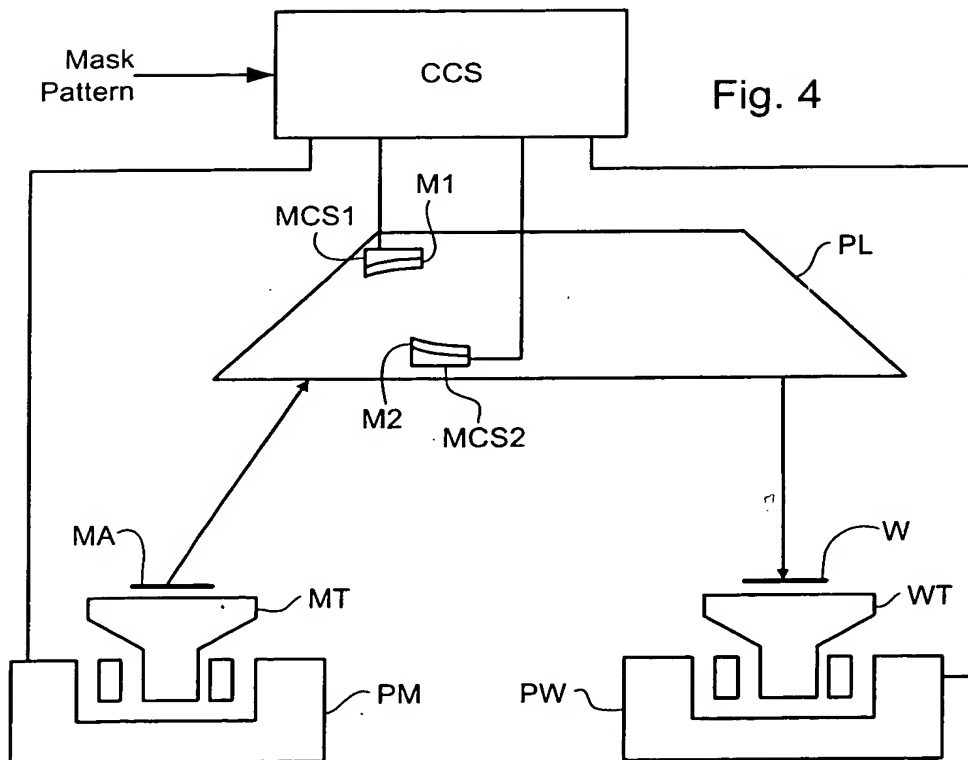


Fig. 5

Addition of aberration to correct for BFshift due to mask :
starting position - 30nm Bright Field

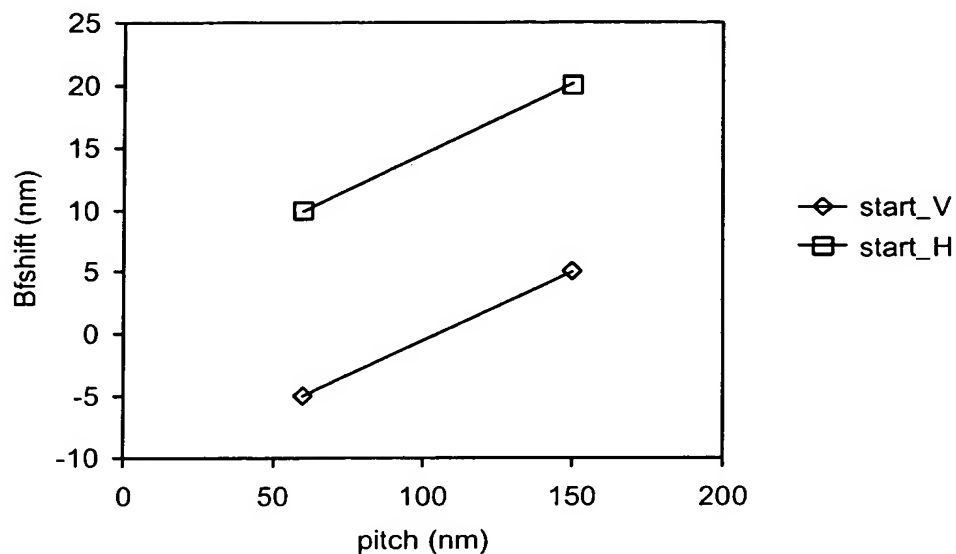


Fig. 6

Effect of BFshift correction on IFT :
starting position - 30nm Bright Field

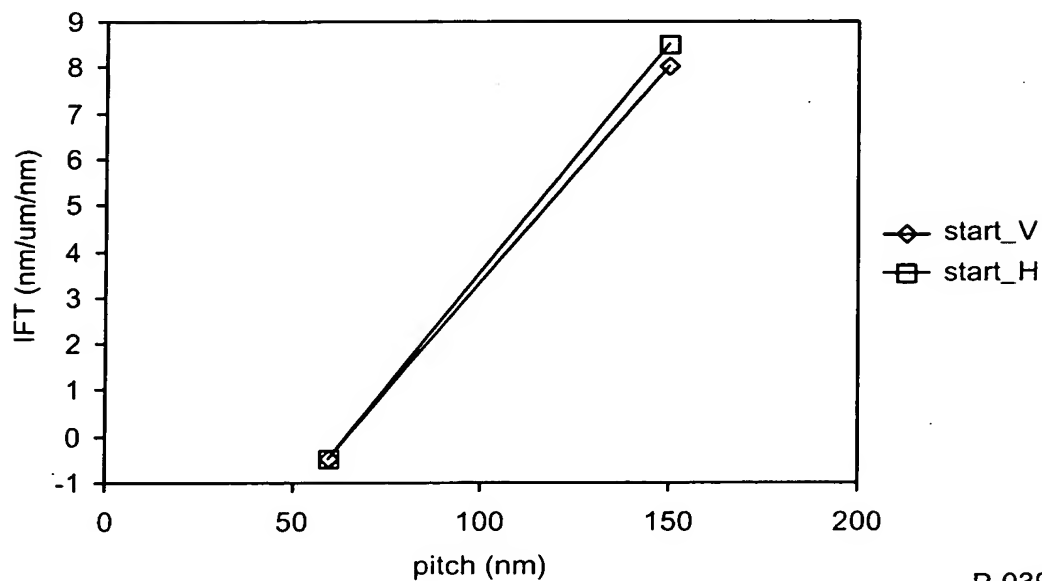


Fig. 7

Addition of aberration to correct for BFshift due to mask :
 Z5-0.26nm and Z9-0.24nm and Z12-0.07nm -30nm Bright Field

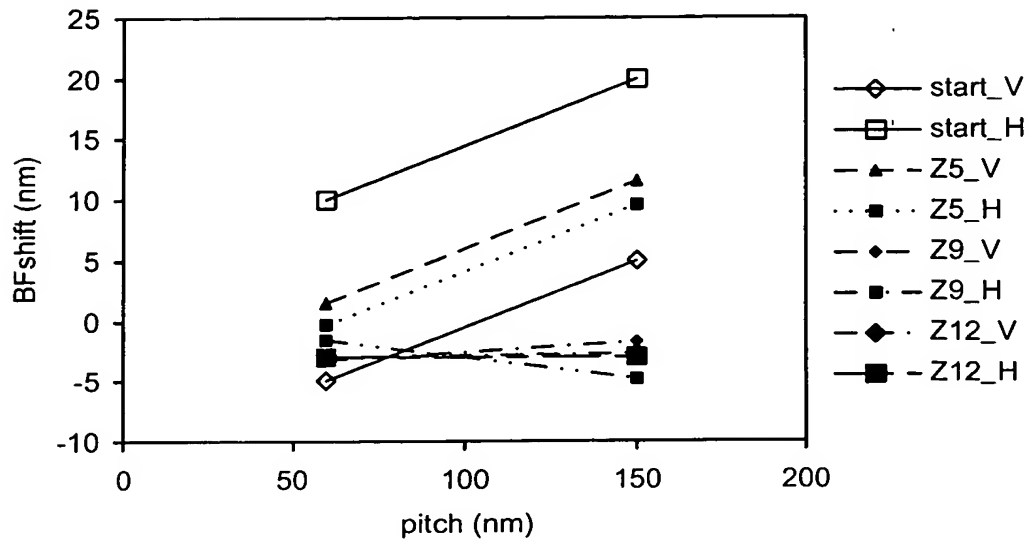


Fig. 8

Effect of BFshift correction on IFT :
 Z5-0.26nm and Z9-0.24nm and Z12-0.07nm - 30nm Bright Field

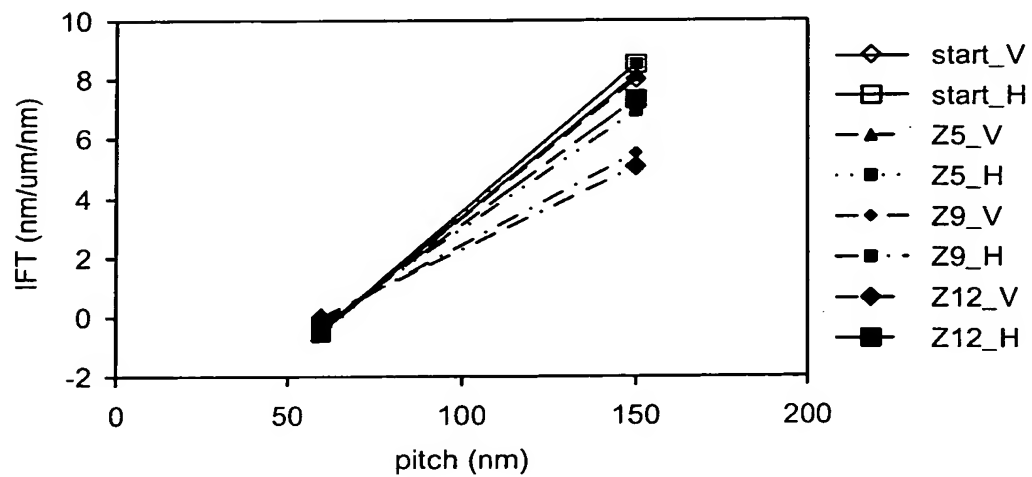


Fig. 9

Addition of aberration to correct for BFshift due to mask :
 Z5-0.18nm and Z9-0.22 and Z12-0.18nm - 50nm Bright Field

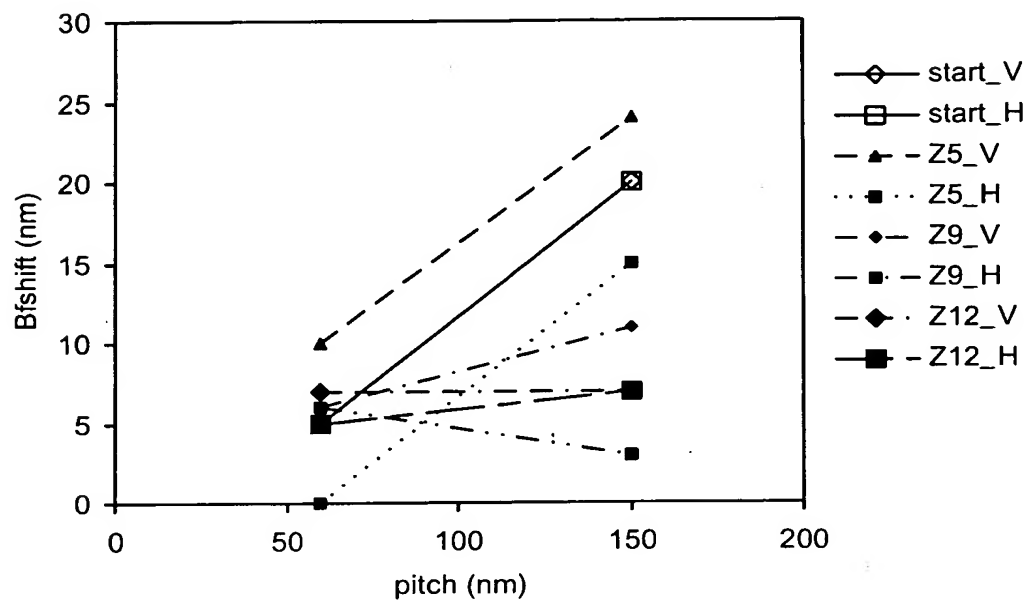


Fig. 10

Correction of IFT without impact on BFshifts :
 Z5-0.4nm and Z9-0.55nm and Z12-0.11nm - 30nm Bright Field

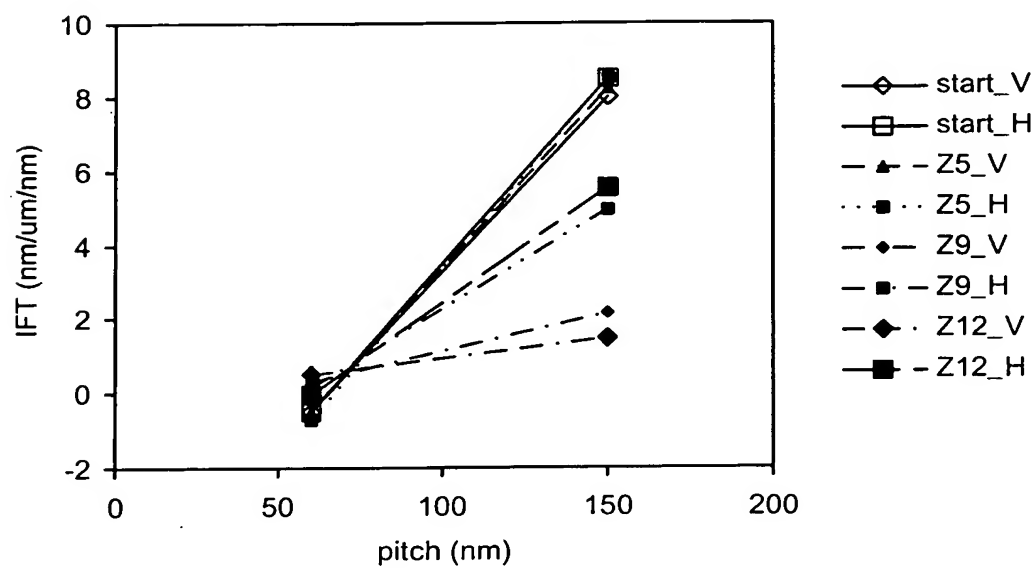


Fig. 11

Correction of IFT without impact on BFshift :
 Z5-0.34nm and Z9-0.11 and Z12-0.37nm - 50nm Bright Field

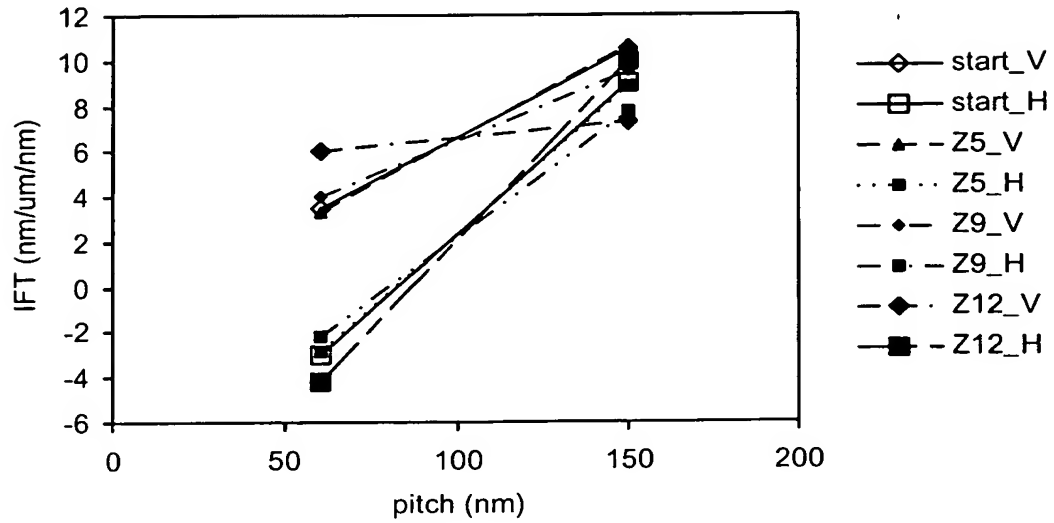


Fig. 12

30nm IL NA/s=0.25/0.5 6 degrees mask incidence
 Solid-EUV & EUV2D

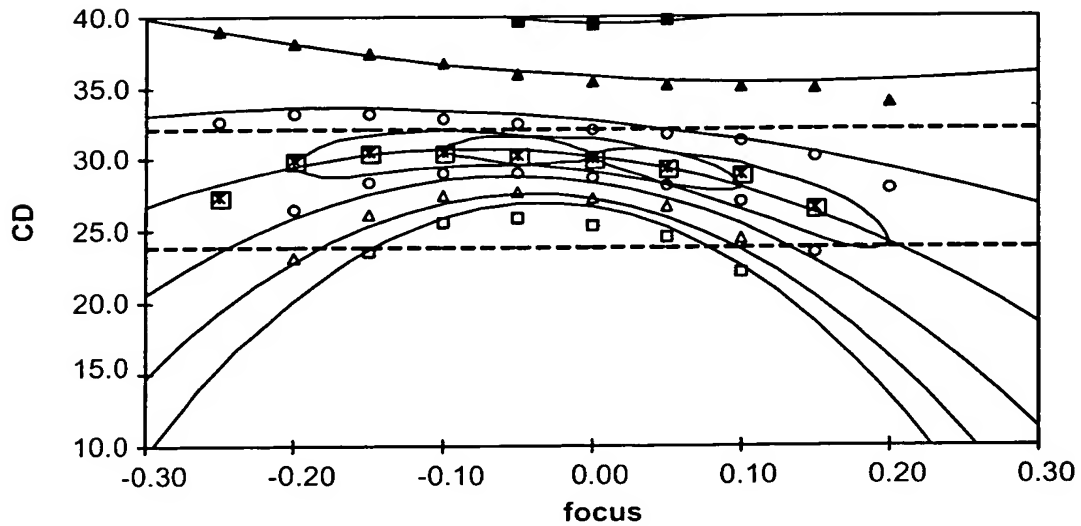


Fig. 13

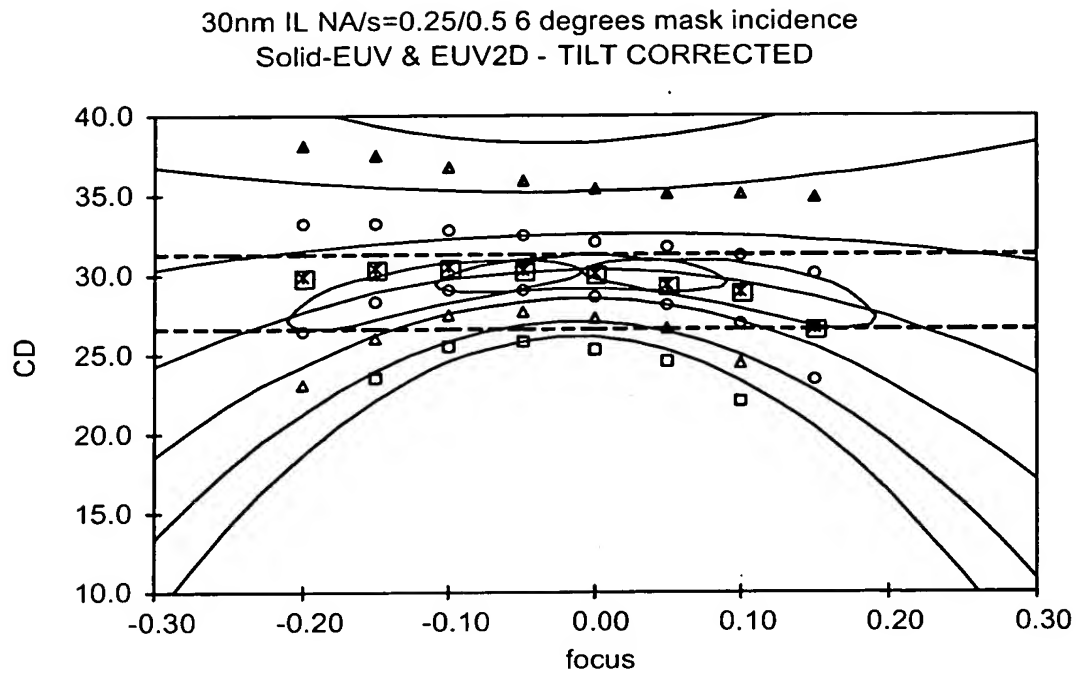


Fig. 14

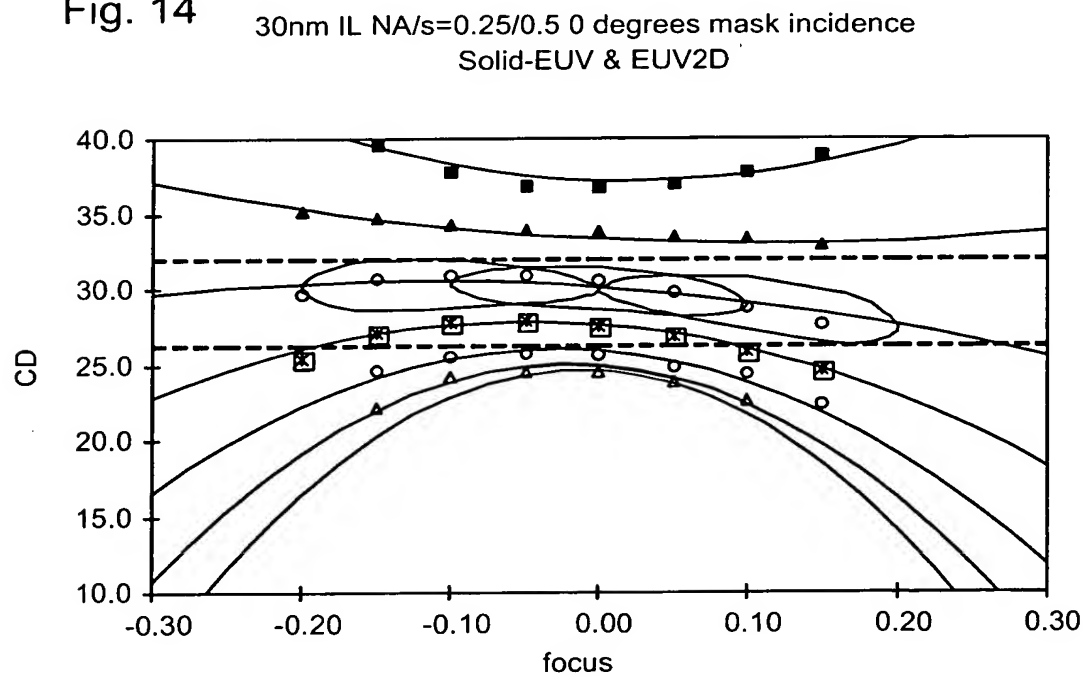


Fig. 15

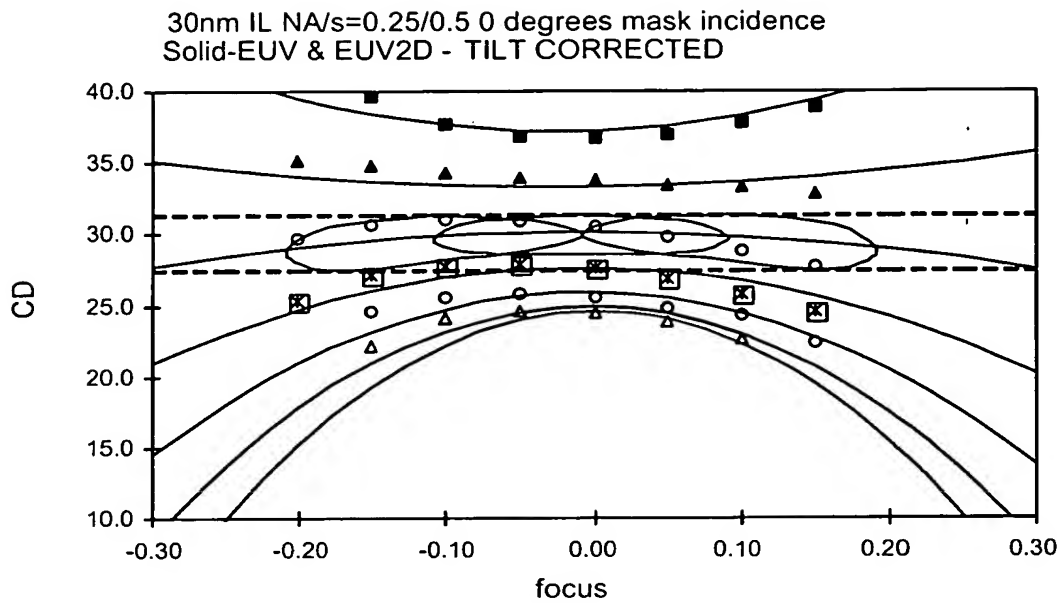


Fig. 16

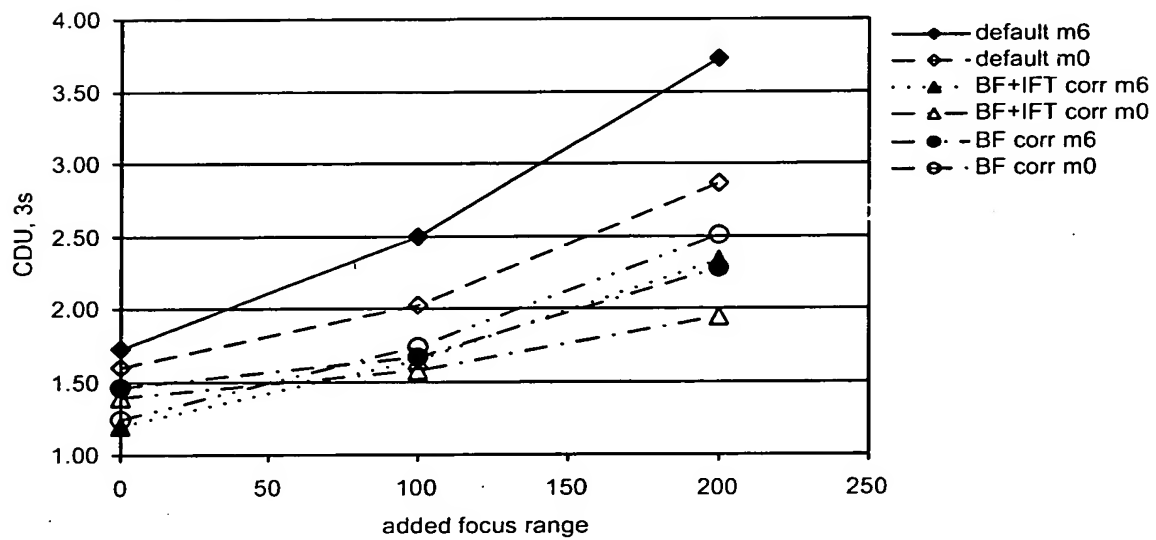


Fig. 17

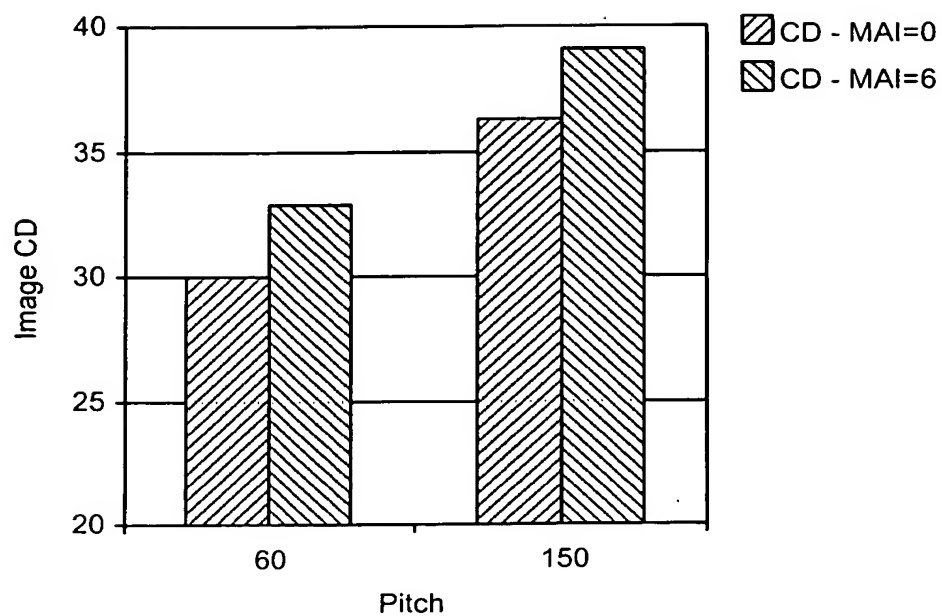


Fig. 18

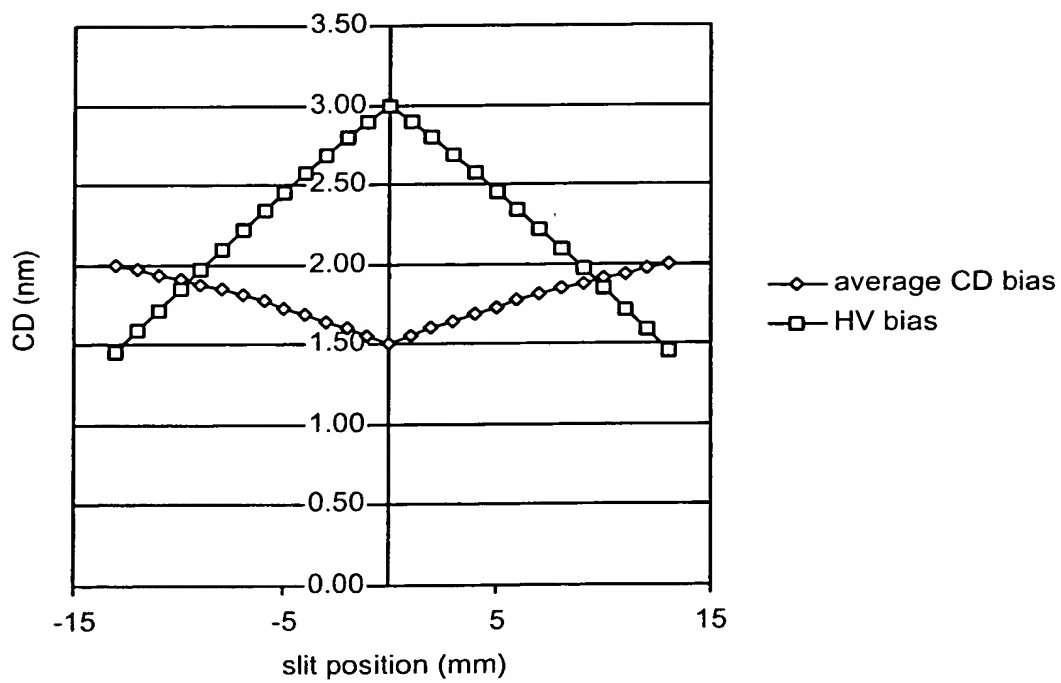


Fig. 19

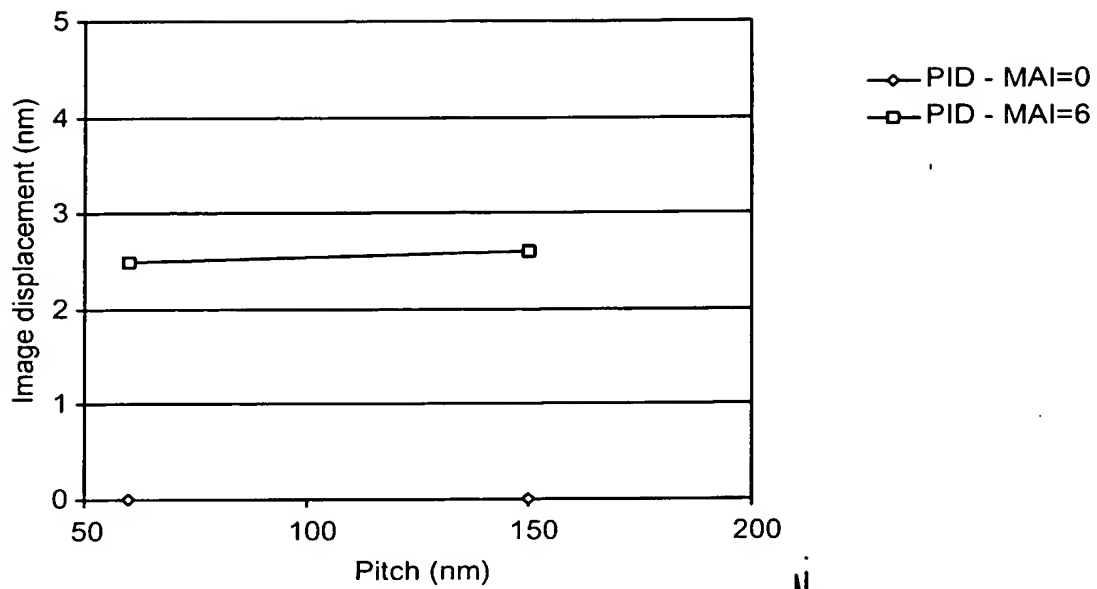


Fig. 20

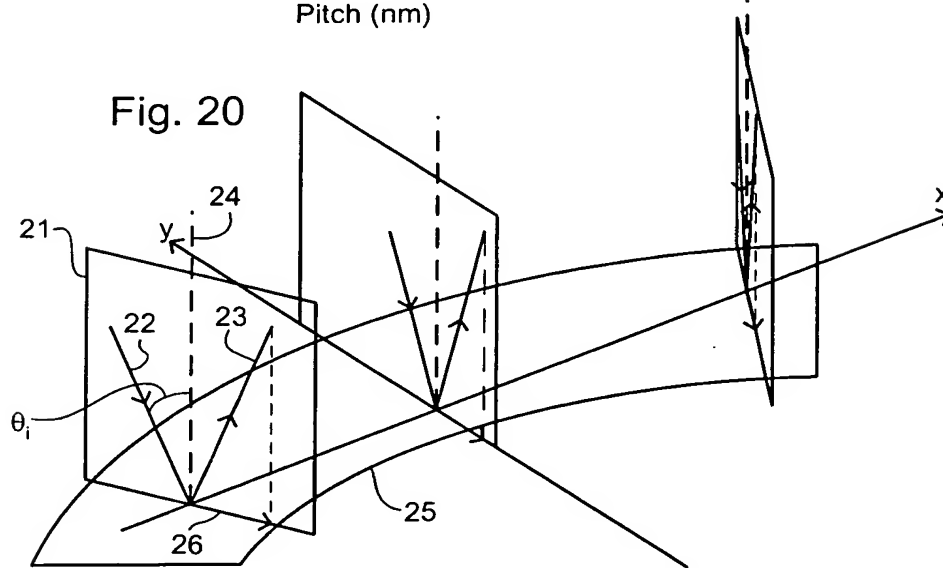


Fig. 22

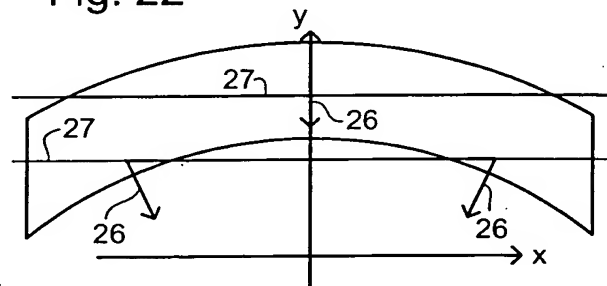
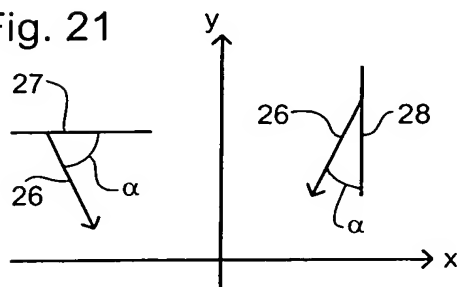


Fig. 21



P-0393